Stem Cell Research 42 (2020) 101667

Contents lists available at ScienceDirect

Stem Cell Research

journal homepage: www.elsevier.com/locate/scr

Lab Resource: Multiple Cell Lines

Generation of two isogenic knockout *PKD2* iPS cell lines, IRFMNi003-A-1 and IRFMNi003-A-2, using CRISPR/Cas9 technology

Piera Trionfini, Osele Ciampi, Elena Romano, Ariela Benigni, Susanna Tomasoni*

Istituto di Ricerche Farmacologiche Mario Negri IRCCS, Centro Anna Maria Astori, Science and Technology Park Kilometro Rosso, Via Stezzano, 87, 24126 Bergamo, Italy

A B S T R A C T

Autosomal dominant polycystic kidney disease (ADPKD) is the most prevalent inherited renal disease, characterized by multiple cysts that can lead to kidney failure resulting in end-stage renal disease. ADPKD is mainly caused by mutations in either the *PKD1* and *PKD2* genes, encoding for polycystin-1 and polycystin-2, respectively. In order to clarify the disease mechanisms, here we describe the generation of two isogenic induced pluripotent stem cell (iPSC) lines in which the *PKD2* gene was deleted using CRISPR/Cas9 technology. The *PKD2*$^{-/-}$ iPSCs expressed the main pluripotency markers, were able to differentiate into the three germ layers and had a normal karyotype.

Resource table

Unique stem cell lines identifier	IRFMNi003-A-1 IRFMNi003-A-2
Alternative names of stem cell lines	KO PKD2#17 (IRFMNi003-A-1) KO PKD2#36 (IRFMNi003-A-2)
Institution	Istituto di Ricerche Farmacologiche Mario Negri IRCCS
Contact information of distributor	Susanna Tomasoni susanna.tomasoni@marionegri.it
Type of cell lines	iPSC
Origin	Human
Cell Source	Peripheral blood mononuclear cells (PBMCs)
Clonality	Clonal
Method of reprogramming	Sendai Virus
Multiline rationale	Isogenic clones
Gene modification	YES
Type of modification	Deletion
Associated disease	Autosomal dominant polycystic kidney disease
Gene/locus	PKD2/4q22.1
Method of modification	CRISPR/Cas9
Name of transgene or resistance	N/A
Inducible/constitutive system	N/A
Date archived/stock date	July 2019
Cell line repository/bank	N/A
Ethical approval	Ethical Committee of Bergamo, Protocol number 58/19

1. Resource utility (Max 50 words)

Knockout *PKD2* iPSC lines, IRFMNi003-A-1 and IRFMNi003-A-2 (Table 1), can be used to investigate the disease mechanisms underlying ADPKD and to develop a novel drug discovery platform.

2. Resource details

ADPKD cystogenesis is a very complicated process and is attributed to loss of function mutations in the *PKD1* and *PKD2* genes that encode polycystin-1 and polycystin-2, respectively. The polycystin complex localizes in the primary cilium in the renal epithelia, where it processes cilium mechanical stimulation, resulting from tubular fluid flow. A high level of allelic heterogeneity is found in all *PKD* genes, and hundreds of unique mutations have been reported (Bergmann et al., 2018). Recently, drug screening using kidney organoids that were generated using *PKD1*$^{-/-}$ and *PKD2*$^{-/-}$ iPSCs, and which are able to reproduce cyst formation *in vitro*, unexpectedly revealed that myosin plays a role in ADPKD pathogenesis (Czerniecki et al., 2018). These results demonstrated the usefulness of generating a *PKD1*$^{-/-}$ and *PKD2*$^{-/-}$ iPSC to model ADPKD *in vitro*. Here, we describe the generation of iPSCs knocked out for the *PKD2* gene, starting from iPSCs derived from the PBMCs of a healthy 32-year old woman (IRFMNi003-A) using Sendai virus technology, as described earlier (Ciampi et al., 2016).

A single guide RNA targeting *PKD2* exon 1 (GCGTGGAGCCGCGATAACCC), previously designed and tested for its cutting efficiency by Freedman (Freedman et al., 2015), was cloned into a plasmid containing Cas9 from S. pyogenes, fused with 2A-EGFP (pSpCAs9(BB)-2A-GFP, PX458; Addgene). IRFMNi003-A cells were nucleofected with pSpCas9(BB)-2A-GFP-sg*PKD2*, followed by fluorescence-activated cell sorting (FACS) of GFP^{+} cells, single cell seeding on a mouse embryonic fibroblast (MEF)-feeder layer and manual picking. Single cell-derived clones were then expanded on matrigel-coated plates and analyzed

* Corresponding author.
E-mail address: susanna.tomasoni@marionegri.it (S. Tomasoni).

https://doi.org/10.1016/j.scr.2019.101667
Received 26 September 2019; Received in revised form 11 November 2019; Accepted 21 November 2019
Available online 29 November 2019

Table 1
Summary of lines.

iPSC line names	Abbreviation in figures	Gender	Age	Ethnicity	Genotype of locus	Disease
IRFMNi003-A-1	KO PKD2#17	Female	32	Caucasian	PKD2 Knockout	Autosomal dominant polycystic kidney disease
IRFMNi003-A-2	KO PKD2#36	Female	32	Caucasian	PKD2 knockout	Autosomal dominant polycystic kidney disease

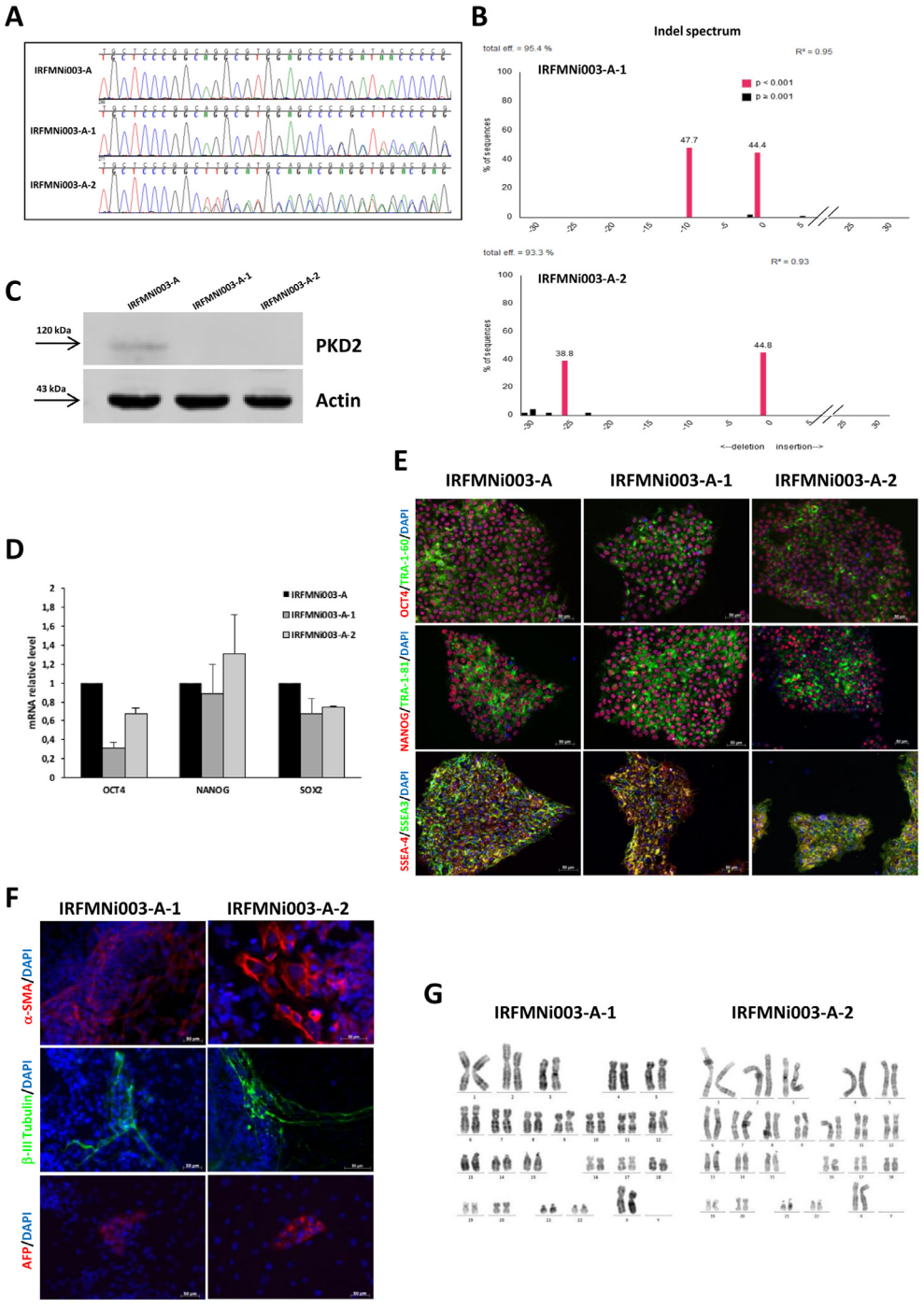

Fig. 1. Characterization of IRFMNi003-A-1 and IRFMNi003-A-2 iPS cell lines.

through Sanger sequencing. We selected two of the 40 analyzed clones, in which NHEJ occurred on both alleles (Fig. 1A and B). Both clones carried a 1 bp deletion (c.276_276delC, p.G93Afs*24) on one allele while on the other allele clone IRFMNi003-A-1 carried a 10 bp deletion (c.266_275delGCGATAACCC, p.R89Pfs*25) and clone IRFMNi003-A-2 carried a 26 bp deletion (c.254_279delAGGCGTGGAGCCGCGATAACC CCGGC, p.Q85Lfs*119) (Fig. 1A and B; Supplementary Fig. 1A). All these frameshift mutations led to the loss of polycystin-2 expression, demonstrated by western blot analysis (Fig. 1C). The top 7 off-target cleavage and those that fell within protein coding regions or next to

Table 2
Characterization and validation.

Classification	Test	Result	Data
Morphology	*Photography*	*Normal*	Supplementary Fig. 1B
Phenotype	Qualitative analysis *by Immunocytochemistry*	*Assess staining of pluripotency markers: OCT4, NANOG, TRA-1-60, TRA-1-81, SSEA-3, SSEA-4*	Fig. 1 panel E
	Quantitative analysis *by RT-qPCR*	*All the cell lines express the pluripotency markers OCT4, NANOG and SOX2 at levels comparable to the parental iPSC line*	Fig. 1 panel D
Genotype	Karyotype (G-banding) and resolution	*46XX, Resolution 400–550*	Fig. 1 panel G
Identity	Microsatellite PCR (mPCR) OR	*N/A*	
	STR analysis	*18 sites tested / Matched*	Submitted in archive with journal
Mutation analysis (IF APPLICABLE)	Sequencing	Compound heterozygous status in both cell lines	Fig. 1 panel A and B Supplementary Fig. 1A
	Southern Blot OR WGS	N/A	N/A
Microbiology and virology	Mycoplasma	*Mycoplasma testing by PCR. Negative*	Supplementary Fig. 1C
Differentiation potential	Embryoid body formation	*Mesoderm: smooth muscle actin* *Ectoderm: β-III-tubulin* *Endoderm α-feto protein*	Fig. 1 panel F
Donor screening (OPTIONAL)	HIV 1 + 2 Hepatitis B, Hepatitis C	*N/A*	*N/A*
Genotype additional info (OPTIONAL)	Blood group genotyping	*N/A*	*N/A*
	HLA tissue typing	*N/A*	*N/A*

intronic-exonic junctions (< 1000 bp) (Supplementary Table 1) were excluded by Sanger sequencing for both clones (data not shown). The knockout clones IRFMNi003-A-1 and IRFMNi003-A-2 exibited normal pluripotent morphology (Supplementary Fig. 1B) and expressed pluripotency markers at the mRNA (Fig. 1D) and protein level (Fig. 1E) at comparable levels to their parental cell line. Moreover, they were able to spontaneously differentiate *in vitro* into derivatives of the three germ layers and had a normal karyotype (Fig. 1F and G, respectively). The edited clones were authenticated using Short Tandem Repeat (STR) analysis, revealing an identical profile to the parental iPSCs (Table 2, data not shown but available from authors). Finally, both clones were confirmed to be mycoplasma-free (Supplementary Fig. 1C).

In summary, we have generated two human compound heterozygous *PKD2*$^{-/-}$ iPSC lines. These will serve as an ideal tool for *in vitro* disease modeling and pathological study of ADPKD.

3. Materials and methods

3.1. Cell culture

The iPSCs were cultured on hES-qualified matrigel-coated plates in mTeSR1 medium (Stemcell Technologies) in a humidified chamber at 37 °C and 5% CO_2. Mouse embryonic fibroblasts (MEFs) were cultured in Dulbecco's modified Eagle's medium (DMEM) containing 10% fetal bovine serum (FBS, Gibco) and 0.1 mM non-essential amino acids (NEAA; Gibco). MEFs were mitotically inactivated through mitomycin c treatment (Sigma-Aldrich) 48 h before iPSC seeding. Mycoplasma contamination was detected using the N-GARDE Mycoplasma Detection PCR Kit (Euroclone).

3.2. CRISPR/Cas9-mediated PKD2 knockout

For *PKD2* knockout, 18×10^6 iPSCs were nucleofected with 72 μg pSpCas9(BB)-2A-GFP-sg*PKD2*. Soon after nucleofection, cells were plated on 6-well matrigel-coated plates in 4 ml mTeSR1 supplemented with 10 μM Y-27632 (Sigma-Aldrich). Twenty-four hours later, cells were detached using Accutase (Gibco) and resuspended (2×10^6 cells/ml) in Hank's Balanced Salt Solution (HBSS, Gibco) supplemented with 4% FBS Hyclone (Euroclone), 10 mM Hepes (Gibco), Pen/Strep, 2 mM EDTA (Gibco) and 10 μM Y-27632. After removing cell clumps and debris through a Filcon filter (BD Biosciences), GFP^+ single cells were isolated through cell sorting (FACSAria IIu; BD Bioscience) and plated at a density of 500 cells/cm^2 on MEF-feeder coated plates to allow single cell clone formation. Eight to ten days later, 40 emergent clones were picked manually and immediately plated on matrigel-coated wells in mTeSR1 medium.

3.3. Genotyping and sequencing

Genomic DNA was extracted from edited clones with the DNeasy Blood and Tissue kit (Qiagen). The *PKD2* gene was amplified by PCR (Long Range DNA Polymerase, biotechrabbit) using the primers listed in Table 3. PCR amplicon was analyzed using Sanger sequencing on the 3730 DNA Analyzer (Applied Biosystem). Hypothesized deletions were disentangled and verified using the TIDE (Tracking of Indels by DEcomposition) online software tool (Fig. 1B) (Brinkman et al., 2014). Amplicons that had frameshift mutations were further confirmed by TOPO TA cloning (Invitrogen) and Sanger sequencing (Supplementary Fig. 1A). The results were aligned using SnapGene software.

3.4. Western blot

Protein lysates (40 μg) were analyzed through sodium dodecyl sulfate polyacrylamide gel electrophoresis on a 8% acrylamide gel under reducing conditions and visualized by immunoblot. The signals were visualized on an Odyssey FC Imaging System (LiCor) through infrared fluorescence. The antibodies used are listed in Table 3.

3.5. Pluripotency gene expression analysis

Total RNA was isolated with Trizol Reagent (Invitrogen) and treated with DNAse (Promega), as instructed by the manufacturer. cDNA was synthetized from 2 μg of total RNA with Vilo Superscript kit (Invitrogen). Quantitative real-time PCR (qRT-PCR) reactions were performed using TaqMan gene expression assays (Applied Biosystems), using predesigned TaqMan probes for the genes of interest according to the supplier's recommendations (Table 3).

3.6. Immunocytochemistry

The cells were fixed with 4% paraformaldehyde (Società Italiana Chimici), permeabilized with 0.3% Triton X-100 (Sigma-Aldrich) for 10 min at room temperature (RT) and then incubated for 1 h with 5% bovine serum albumin (BSA, Sigma-Aldrich) as a blocking solution. Primary antibodies were applied overnight at 4 °C, followed by incubation with the appropriate secondary antibody for 1 h at RT. Nuclei were counterstained with 4′,6-diamidino-2-phenylindole (DAPI, Sigma-Aldrich). Images were taken using the Axio Observer Z1 fluorescence

Table 3
Reagents details.

Antibodies used for immunocytochemistry/flow-cytometry			
	Antibody	**Dilution**	**Company Cat # and RRID**
Pluripotency Markers	*Mouse anti-OCT4*	1:100	*Santa Cruz Biotechnology Cat# sc-5279; RRID: AB_628051*
	Rabbit anti-NANOG	1:100	*Santa Cruz Biotechnology Cat# sc-33759; RRID: AB_2150401*
	Mouse anti–TRA–1–60	1:200	*Millipore Cat# MAB4360; RRID: AB_2119183*
	Mouse anti–TRA–1–81	1:200	*Millipore Cat# MAB4381; RRID: AB_177638*
	Mouse anti-SSEA-4	1:100	*Santa Cruz Biotechnology Cat# sc-21704;RRID: AB_628289*
	Rat anti-SSEA-3	1:100	*Santa Cruz Biotechnology Cat# sc-21703;RRID: AB_628288*
Differentiation Markers	*Mouse anti-Tubulin beta-III, clone TU-20, Alexa Fluor 488 Conjugated*	1:100	*Millipore Cat# CBL412X; RRID: AB_1977541*
	Mouse anti-Actin, alpha-Smooth Muscle - Cy3	1:100	*Sigma-Aldrich Cat# C6198; RRID: AB_476856*
	AFP (AFP-11) antibody	1:100	*Santa Cruz Biotechnology Cat# sc-51506;RRID: AB_626514*
Secondary antibodies	*Donkey anti-Rabbit IgG (H + +L) Highly Cross-Adsorbed Secondary Antibody, Alexa Fluor 546*	1:300	*Thermo Fisher Scientific Cat# A10040; RRID: AB_2534016*
	Goat anti-Mouse IgM Heavy Chain Cross-Adsorbed Secondary Antibody, Alexa Fluor 488	1:300	*Thermo Fisher Scientific Cat# A-21042;RRID: AB_2535711*
	Donkey anti-Mouse IgG (H + +L) Highly Cross-Adsorbed Secondary Antibody, Alexa Fluor 546	1:300	*Thermo Fisher Scientific Cat# A10036; RRID: AB_2534012*
	*Alexa Fluor 488 goat anti-rat IgM (micro chain) *2 mg mL* antibody*	1:300	*Thermo Fisher Scientific Cat# A-21212; RRID: AB_2535798*
Western blot antibodies	*Mouse anti-Polycystin-2 (D-3)*	1:200	*Santa Cruz Biotechnology Cat# sc-28331;RRID: AB_672377*
	Rabbit Anti-Actin (20–33) antibody	1:3000	*(Sigma-Aldrich Cat# A5060; RRID:AB_476738)*
	Goat Anti-Mouse IgG Antibody, IRDye® 680LT Conjugated	1:10,000	*LI-COR Biosciences Cat# 926-68020;RRID:AB_10706161*
	Goat Anti-Rabbit IgG, IRDye® 800CW Conjugated antibody	1:10,000	*LI-COR Biosciences Cat# 926-32211;RRID:AB_621843*
Primers			
	Target	**Forward/Reverse primer (5′ – 3′)**	
Pluripotency Markers (qPCR)	*NANOG*	*Hs02387400_g1 (Thermo Fisher Scientific)*	
	OCT4	*Hs00742896_s1 (Thermo Fisher Scientific)*	
	SOX2	*Hs00602736_s1 (Thermo Fisher Scientific)*	
House-Keeping Genes (qPCR)	*HPRT1*	*Hs99999909_m1 (Thermo Fisher Scientific)*	
Genotyping	*PKD2*	*Fwd: CTTGGAACGCGGACTCGG / Rev: GGGTACCGGAAATAGGGCAG*	
Targeted mutation sequencing	*PKD2*	*Fwd: GTGACCGCGATGGTGAACTCCAG / Rev: GCGGAACGCAGAGGGGATGCGA*	

microscope (Zeiss). The antibodies used are listed in Table 3.

3.7. Embryoid body (EB) formation

The iPSCs were detached using dispase (Stemcell Technologies) and transferred into an Ultra Low-attach six well-plate in DMEM/F-12 medium, supplemented with 20% KO serum (Gibco), 0.1 mM 2-mercaptoethanol (Gibco), 1X NEAA plus 10 μM Y-27,632. Forty-eight hours after plating, Y-27,632 was removed and EBs were cultured for another 6 days as a floating culture. Thereafter, EBs were then transferred onto a gelatin-coated plate for another 8 days.

3.8. Karyotyping and cell authentication

Karyotype analysis was performed in collaboration with the Genetic Medicine Laboratory of the Azienda Socio Sanitaria Territoriale Papa Giovanni XXIII, Bergamo (Italy). Metaphase spreads were prepared after 3 h treatment with Colcemid (Roche) and processed for karyotype analysis. A minimum of 20 metaphases were analyzed. Cell line authentication was performed using the ATCC Human Short Tandem Repeat (STR) Profiling Cell Authentication Service.

Declarations of Competing Interest

None.

Acknowledgments

The authors are grateful to Paolo Fruscella and Ursula Giussani for performing the karyotype analysis, to Marta Alberti and Marta Todeschini for technical assistance and to Kerstin Mierke for English language editing. E.R. is the recipient of a fellowship from Fondazione Aiuti per la Ricerca sulle Malattie Rare (ARMR), Bergamo, Italy.

Supplementary materials

Supplementary material associated with this article can be found, in the online version, at doi:10.1016/j.scr.2019.101667.

References

Bergmann, C., Guay-Woodford, L.M., Harris, P.C., Horie, S., Peters, D.J.M., Torres, V.E., 2018. Polycystic kidney disease. Nat. Rev. Dis. Primer 4, 50. https://doi.org/10.1038/s41572-018-0047-y.

Brinkman, E.K., Chen, T., Amendola, M., van Steensel, B., 2014. Easy quantitative assessment of genome editing by sequence trace decomposition. Nucleic Acids Res. 42, e168. https://doi.org/10.1093/nar/gku936.

Ciampi, O., Iacone, R., Longaretti, L., Benedetti, V., Graf, M., Magnone, M.C., Patsch, C., Xinaris, C., Remuzzi, G., Benigni, A., Tomasoni, S., 2016. Generation of functional podocytes from human induced pluripotent stem cells. Stem Cell Res. 17, 130–139. https://doi.org/10.1016/j.scr.2016.06.001.

Czerniecki, S.M., Cruz, N.M., Harder, J.L., Menon, R., Annis, J., Otto, E.A., Gulieva, R.E., Islas, L.V., Kim, Y.K., Tran, L.M., Martins, T.J., Pippin, J.W., Fu, H., Kretzler, M., Shankland, S.J., Himmelfarb, J., Moon, R.T., Paragas, N., Freedman, B.S., 2018. High-Throughput screening enhances kidney organoid differentiation from human pluripotent stem cells and enables automated multidimensional phenotyping. Cell Stem Cell 22, 929–940. https://doi.org/10.1016/j.stem.2018.04.022. e4.

Freedman, B.S., Brooks, C.R., Lam, A.Q., Fu, H., Morizane, R., Agrawal, V., Saad, A.F., Li, M.K., Hughes, M.R., Werff, R.V., Peters, D.T., Lu, J., Baccei, A., Siedlecki, A.M., Valerius, M.T., Musunuru, K., McNagny, K.M., Steinman, T.I., Zhou, J., Lerou, P.H., Bonventre, J.V., 2015. Modelling kidney disease with CRISPR-mutant kidney organoids derived from human pluripotent epiblast spheroids. Nat. Commun. 6, 8715. https://doi.org/10.1038/ncomms9715.